Supporting Information

Electronic effects of transition metal dopant Fe(100) and Fe_5C_2(100) surfaces for CO activation

Huiyong Gong, [abc] *Yurong He*[d] *Junqing Yin,* [abc] *Suyao Liu,*[b] *Ming Qing,*[b] *Qing Peng,*[e] *Chun-Fang Huo,*[b] *Hong Wang,**[b] *Yong Yang,**[abc] *Xiao-Dong Wen**[abc]

a) State Key Laboratory of Coal Conversion, Institute of Coal Chemistry, Chinese Academy of Sciences, Taiyuan, 030001, China; b) National Energy Center for Coal to Liquids, Synfuels China Co., Ltd, Huairou District, Beijing, 101400, China; c) University of Chinese Academy of Sciences, No.19A Yuquan Road, Beijing, 100049, P. R. China; d) Beijing Advanced Innovation Center for Materials Genome Engineering, Beijing Information S & T University, Beijing, 101400, China; e) Nuclear Engineering and Radiological Sciences, University of Michigan, Ann Arbor, MI 48109 (USA)

Corresponding Authors: Hong Wang (wanghong@synfuelschina.com.cn) Yong Yang (yyong@sxicc.ac.cn) Xiao-Dong Wen (wxd@sxicc.ac.cn)

Table of Content

Table S1. The adsorption energy (Eads/eV), dissociation barrier (Ea/eV) and dissociation energy (ΔE/eV) of CO before and after zero point energy corrections on doped Fe(100) and Fe_5C_2(100) surfaces

	E_{ads}	E_{ads}-ZPE	E_{Δ}	E_a	E_a-ZPE	E_{Δ}	ΔE	ΔE-ZPE	E_{Δ}
Fe(100)–Cr	–2.45	–2.39	0.06	0.87	0.83	–0.04	–0.99	–1.13	–0.04
Fe(100)–Mn	–2.31	–2.26	0.05	0.92	0.90	–0.02	-0.91	–0.93	–0.02
Fe(100)–Fe	–2.25	–2.20	0.05	1.09	1.06	–0.03	–0.85	–0.89	–0.04
Fe(100)–Co	–2.24	–2.19	0.05	1.13	1.10	–0.03	–0.82	–0.85	–0.03
Fe(100)–Ni	–2.14	–2.09	0.05	1.17	1.14	–0.03	–0.77	–0.81	–0.04
Fe(100)–Cu	–1.94	–1.90	0.04	1.22	1.20	–0.02	–0.73	–0.76	–0.03

	E_{ads}	E_{ads}-ZPE	E_{Δ}	E_a	E_a-ZPE	E_{Δ}	ΔE	ΔE-ZPE	E_{Δ}
Fe_5C_2(100)–Cr	–2.83	–2.77	0.07	0.48	0.45	–0.03	–0.75	–0.77	–0.02
Fe_5C_2(100)–Mn	–2.41	–2.35	0.06	0.69	0.65	–0.04	0.03	0.01	–0.02
Fe_5C_2(100)–Fe	–2.26	–2.20	0.06	0.77	0.73	–0.04	0.27	0.24	–0.03
Fe_5C_2(100)–Co	–2.09	–2.05	0.04	0.91	0.88	–0.03	0.36	0.35	–0.01
Fe_5C_2(100)–Ni	–1.91	–1.86	0.05	0.98	0.95	–0.03	0.52	0.50	–0.02
Fe_5C_2(100)–Cu	–1.75	–1.70	0.05	1.12	1.09	–0.03	0.86	0.84	–0.02

Table S2. Optimized geometry parameters (Å) of adsorbed CO molecule toward M–atom on pure and M–doped Fe(100) (M = Cr / Mn / Co / Ni / Cu) surfaces

surfaces	state	C-O(A)	O-M(A)	O-Fe(A)				C-M(A)	C-Fe(A)		
Fe(100)-Cr	IS	1.331	2.073	2.135				2.310	2.184	1.912	1.951
	TS	1.899	1.887	1.885				2.261	2.037	1.872	1.894
	FS	3.089	1.999	1.991	2.038	2.251		2.115	1.966	1.898	1.915
Fe(100)-Mn	IS	1.329	2.118	2.120				2.395	2.159	1.903	1.962
	TS	1.897	1.832	1.947				2.253	2.054	1.870	1.899
	FS	3.095	2.022	1.994	2.041	2.224		2.087	1.975	1.907	1.922
Fe(100)-Fe	IS	1.317	2.126	2.125				2.205	2.204	1.950	1.949
	TS	1.936	1.889	1.889				2.067	2.067	1.895	1.895
	FS	3.048	2.131	1.995	1.994	2.136		1.979	1.978	1.905	1.905
Fe(100)-Co	IS	1.308	2.211	2.088				2.167	2.242	1.974	1.938
	TS	1.948	1.919	1.853				2.018	2.094	1.915	1.897
	FS	3.082	2.488	1.987	1.956	2.079		1.964	1.967	1.916	1.909
Fe(100)-Ni	IS	1.312		2.088		2.184		1.947	2.209	2.169	1.925
	TS	1.950	1.958	1.822				1.994	2.084	1.920	1.903
	FS	3.143	2.460	1.994	1.926	2.048		1.974	1.954	1.924	1.916
Fe(100)-Cu	IS	1.288		2.036		2.666		2.292	2.278	2.049	1.895
	TS	1.989	2.026	1.794				2.186	2.038	1.879	1.893
	FS	3.202	2.494	2.002	1.923	2.057		2.100	1.949	1.907	1.919

Table S3. Energetic parameter of CO dissociation toward M–atom on pure and M–doped Fe(100) (M = Cr / Mn / Co / Ni / Cu/) surfaces

surface	E_{ads}(IS)/eV	E_{ads}(FS)/eV	E_a/eV	ΔE/eV
Fe(100)–Cr	–2.45	–3.44	0.87	–0.99
Fe(100)–Mn	–2.31	–3.22	0.92	–0.91
Fe(100)–Fe	–2.25	–3.10	1.09	–0.85
Fe(100)–Co	–2.15	–2.93	1.24	–0.78
Fe(100)–Ni	–2.15	–2.77	1.50	–0.62
Fe(100)–Cu	–1.94	–2.59	1.54	–0.66

Table S4. Optimized geometry parameters (Å) of the adsorbed CO molecule away from M–atom on pure and M–doped Fe(100) (M = Cr / Mn / Co / Ni / Cu) surfaces

surfaces	state	C-O(A)	O-M(A)	O-Fe(A)				C-M(A)	C-Fe(A)		
Fe(100)-Cr	IS	1.324		2.125		2.096		2.096	2.150	2.149	1.959
	TS	1.943		1.894		1.877		2.033	2.061	2.025	1.899
	FS	3.018		2.164	1.994	1.985	2.143	2.079	1.975	1.940	1.905
Fe(100)-Mn	IS	1.320		2.102		2.118		2.077	2.171	2.148	1.935
	TS	1.942		1.902		1.870		2.014	2.062	2.029	1.892
	FS	3.033		2.166	2.000	1.992	2.117	1.965	1.957	1.983	1.889
Fe(100)-Fe	IS	1.317	2.126	2.125				2.205	2.204	1.950	1.949
	TS	1.936	1.889	1.889				2.067	2.067	1.895	1.895
	FS	3.048	2.131	1.995	1.994	2.136		1.979	1.978	3.048	2.131
Fe(100)-Co	IS	1.314		2.107		2.153		1.928	2.213	2.198	1.941
	TS	1.959		1.902		1.867		1.865	2.029	2.151	1.891
	FS	3.074		2.149	2.003	1.995	2.146	1.898	1.966	1.994	1.901
Fe(100)-Ni	IS	1.314		2.088		2.172		1.948	2.205	2.174	1.926
	TS	1.968		1.916		1.852		1.869	2.012	2.163	1.887
	FS	3.062		2.169	2.013	1.993	2.133	1.913	1.957	1.989	1.905
Fe(100)-Cu	IS	1.287		2.037		2.638		2.283	2.280	2.054	1.891
	TS	1.947		1.926		1.851		1.973	2.007	2.084	1.883
	FS	3.023		2.203	2.003	1.981	2.114	2.022	1.954	1.956	1.893

Table S5. Energetic parameter of CO dissociation away from M–atom on pure and M–doped Fe(100) (M = Cr / Mn / Co / Ni / Cu) surfaces

surfaces	E_{ads}(IS)/eV	E_{ads}(FS)/eV	E_a/eV	ΔE/eV
Fe(100)–Cr	–2.32	–3.21	1.08	–0.89
Fe(100)–Mn	–2.27	–3.11	1.09	–0.84
Fe(100)–Fe	–2.25	–3.10	1.09	–0.85
Fe(100)–Co	–2.24	–3.05	1.13	–0.82
Fe(100)–Ni	–2.14	–2.91	1.17	–0.77
Fe(100)–Cu	–1.94	–2.67	1.22	–0.73

Table S6. Summary of optimized geometry parameters (Å) of the adsorbed CO molecule on pure and M–doped Fe(100) (M = Cr / Mn / Co / Ni / Cu) surfaces

surfaces	state	C-O(A)	O-M(A)	O-Fe(A)				C-M(A)	C-Fe(A)		
Fe(100)-Cr	IS	1.330	2.072	2.135				2.306	2.181	1.914	1.951
	TS	1.897	1.832	1.947				2.253	2.054	1.870	1.899
	FS	3.087	2.001	1.992	2.045	2.24		2.114	1.966	1.898	1.914
Fe(100)-Mn	IS	1.338	1.977	2.176				2.085	2.214	1.962	1.974
	TS	1.843	1.797	1.966				1.997	2.128	1.915	1.901
	FS	3.002	1.912	1.957	2.064	2.372		1.873	2.016	1.952	1.930
Fe(100)-Fe	IS	1.317	2.126	2.125				2.205	2.204	1.950	1.949
	TS	1.936	1.889	1.889				2.067	2.067	1.895	1.895
	FS	3.048	2.131	1.995	1.994	2.136		1.979	1.978	1.905	1.905
Fe(100)-Co	IS	1.314		2.107		2.153		1.928	2.213	2.198	1.941
	TS	1.959		1.902		1.867		1.865	2.029	2.151	1.891
	FS	3.074		2.149	2.003	1.995	2.146	1.898	1.966	1.964	1.901
Fe(100)-Ni	IS	1.314		2.088		2.172		1.948	2.205	2.174	1.926
	TS	1.968		1.916		1.852		1.869	2.012	2.163	1.887
	FS	3.062		2.169	2.013	1.993	2.133	1.913	1.957	1.989	1.905
Fe(100)-Cu	IS	1.287		2.037		2.638		2.283	2.280	2.054	1.891
	TS	1.947		1.926		1.851		1.973	2.007	2.084	1.883
	FS	3.023		2.203	2.003	1.981	2.114	2.022	1.954	1.956	1.893

Table S7. The integrated overlap populations up to Femi level (ICOHP) of C–O, M–C and M–O bonding of CO adsorption IS for pure and M–doped Fe(100) (M = Cr / Mn / Co / Ni / Cu) surfaces

	Fe(100) –Cr	Fe(100) –Mn	Fe(100) –Fe	Fe(100) –Co	Fe(100) –Ni	Fe(100) –Cu
ICOHP (C–O)	–10.33	–10.35	–10.86	–10.99	–10.95	–11.94
ICOHP (M–C)	–6.27	–6.38	–6.14	–6.07	–5.99	–5.48
ICOHP (M–O)	–2.31	–2.25	–1.58	–1.56	–1.56	–1.20

Table S8. Optimized geometry parameters (Å) of the adsorbed CO molecule on pure and M–doped $Fe_5C_2(100)$ (M = Cr / Mn / Co / Ni / Cu) surfaces

surfaces	state	q-bader/CO	C-O(A)	O-M(A)	O-Fe(A)		C-M(A)	C-Fe(A)		
$Fe_5C_2(100)$-Cr	IS	0.1411	1.342	2.016	2.06		2.25	2.242	1.844	1.868
	TS		1.77	1.808	1.99		1.988	2.027	1.847	1.862
	FS		2.935	1.591	3.17		1.956	1.928	1.908	1.883
$Fe_5C_2(100)$-Mn	IS	0.1768	1.34	2.035	2.05		2.163	2.127	1.872	1.902
	TS	/	1.864	1.875	1.89		1.997	1.996	1.844	1.859
	FS	/	2.824	1.77	2.05	2.022	1.92	1.961	1.859	1.856
$Fe_5C_2(100)$-Fe	IS	0.1264	1.331	2.057	2.06		2.136	2.142	1.869	1.902
	TS	/	1.882	1.876	1.89		1.967	1.999	1.841	1.858
	FS	/	2.832	1.807	2.02	1.982	1.921	1.956	1.85	1.849
$Fe_5C_2(100)$-Co	IS	0.084	1.321	2.083	2.05		2.125	2.139	1.878	1.899
	TS	/	1.896	1.883	1.86		1.947	1.982	1.849	1.856
	FS	/	2.851	1.826	1.99	1.942	1.906	1.955	1.848	1.841
$Fe_5C_2(100)$-Ni	IS	0.0515	1.316	2.131	2.04		2.141	2.143	1.88	1.9
	TS	/	1.907	1.921	1.82		1.944	1.974	1.853	1.856
	FS	/	2.88	1.871	1.96	1.922	1.942	1.944	1.844	1.832
$Fe_5C_2(100)$-Cu	IS	0.0223	1.307	2.214	2.05		2.744	2.197	1.86	1.895
	TS	/	1.957	1.954	1.81		2.091	1.962	1.835	1.838
	FS	/	2.893	1.93	1.94	1.917	2.012	1.923	1.831	1.832

Table S9. The integrated overlap populations up to Femi level (ICOHP) of C–O, M–C and M–O bonding of CO adsorption IS for pure and M–doped $Fe_5C_2(100)$ (M = Cr / Mn / Co / Ni / Cu) surfaces

	$Fe_5C_2(100)$ –Cr	$Fe_5C_2(100)$ –Mn	$Fe_5C_2(100)$ –Fe	$Fe_5C_2(100)$ –Co	$Fe_5C_2(100)$ –Ni	$Fe_5C_2(100)$ –Cu
ICOHP (C–O)	–11.80	–11.94	–12.21	–12.51	–12.62	–12.73
ICOHP (M–C)	–8.82	–8.90	–8.85	–8.74	–8.65	–8.27
ICOHP (M–O)	–3.42	–2.76	–2.51	–2.29	–2.10	–1.86

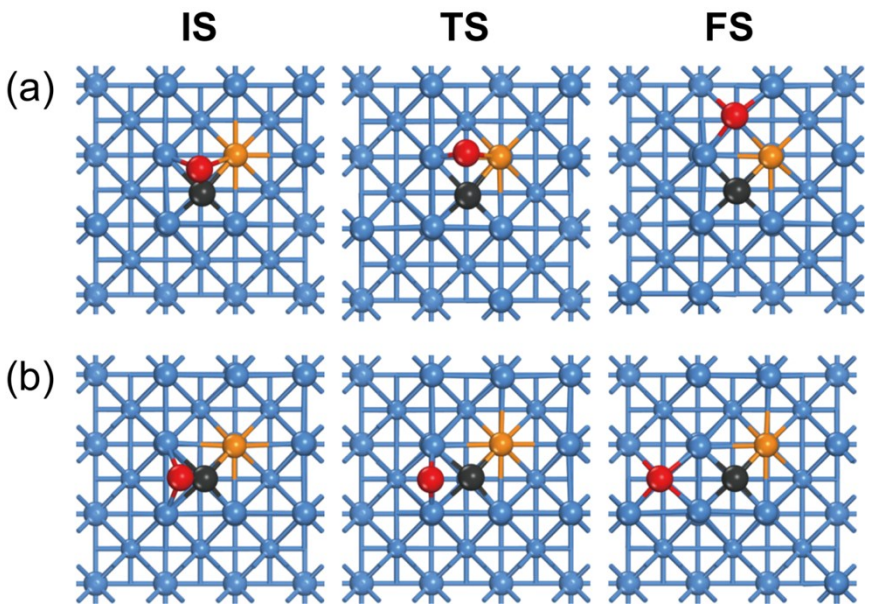

Fig. S1 Paths of CO dissociation on Fe(100)–M surfaces, (a) toward M–atoms; (b) away from M–atoms. Black spheres for C, red spheres for O, blue spheres for Fe, and orange color spheres for the substitution M atoms

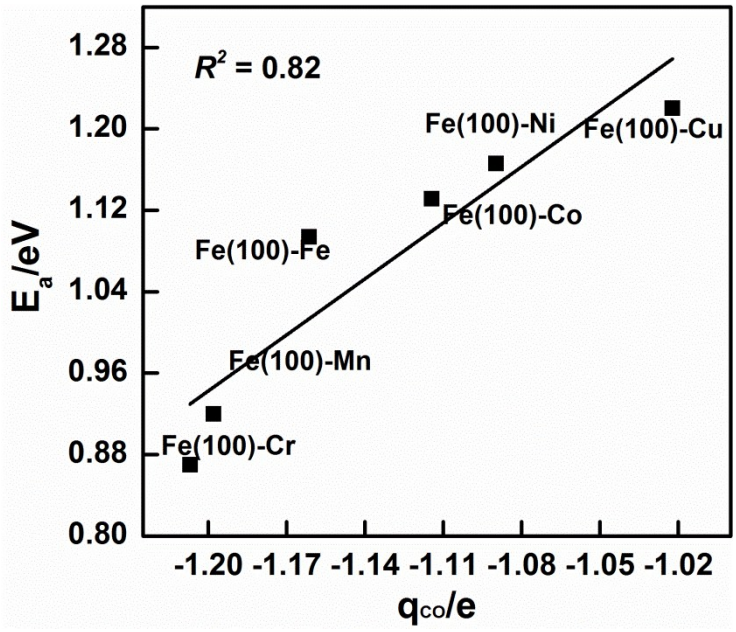

Fig. S2 The relationship between activation barrier (E_a) and the Bader charge (q_{co}) absorbed CO on pure and doped Fe(100) surfaces

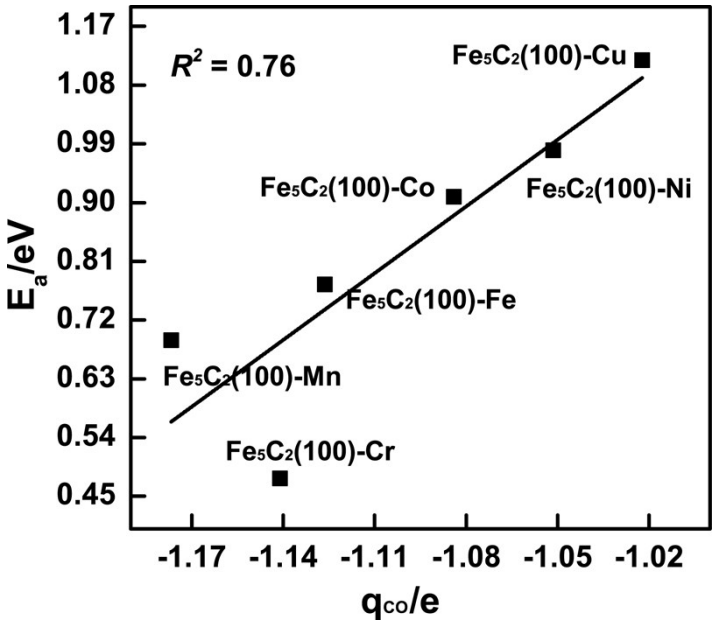

Fig. S3 The relationship between activation barrier (E_a) and the Bader charge (q_{co}) absorbed CO on pure and doped Fe_5C_2(100) surfaces

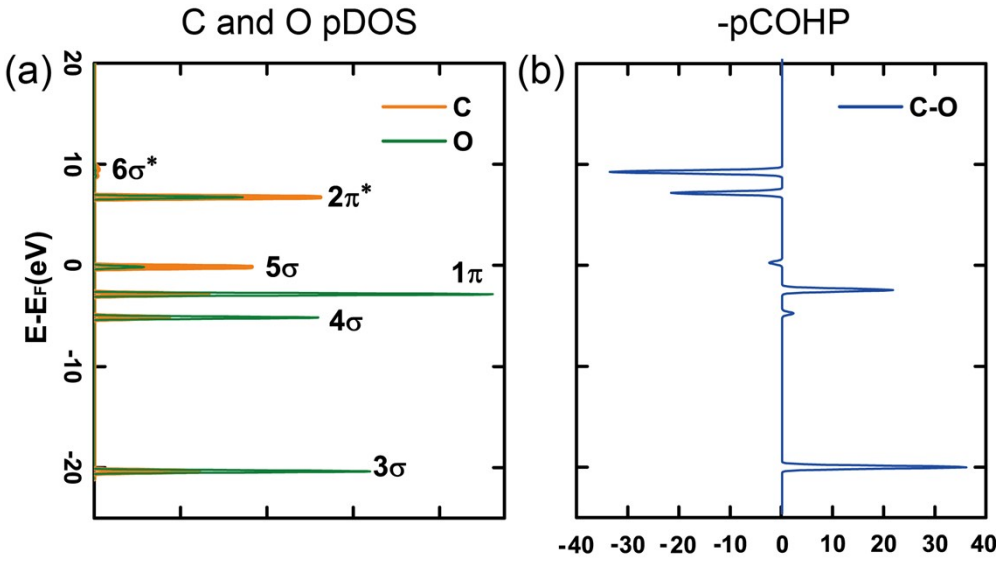

Fig. S4 PDOS and pCOHP curves for free CO. (a) pDOS; (b) pCOHP

The pDOS of free CO molecular and the pCOHP curves for the C–O pair are displayed in **Fig. S4**. The pCOHP analysis shows that 3σ and 1π orbital contribute to the bonding mainly, which are both polarized toward the oxygen atom in pDOS curves. We also see that the 4σ and 5σ orbital are only slightly contributed to the bonding.

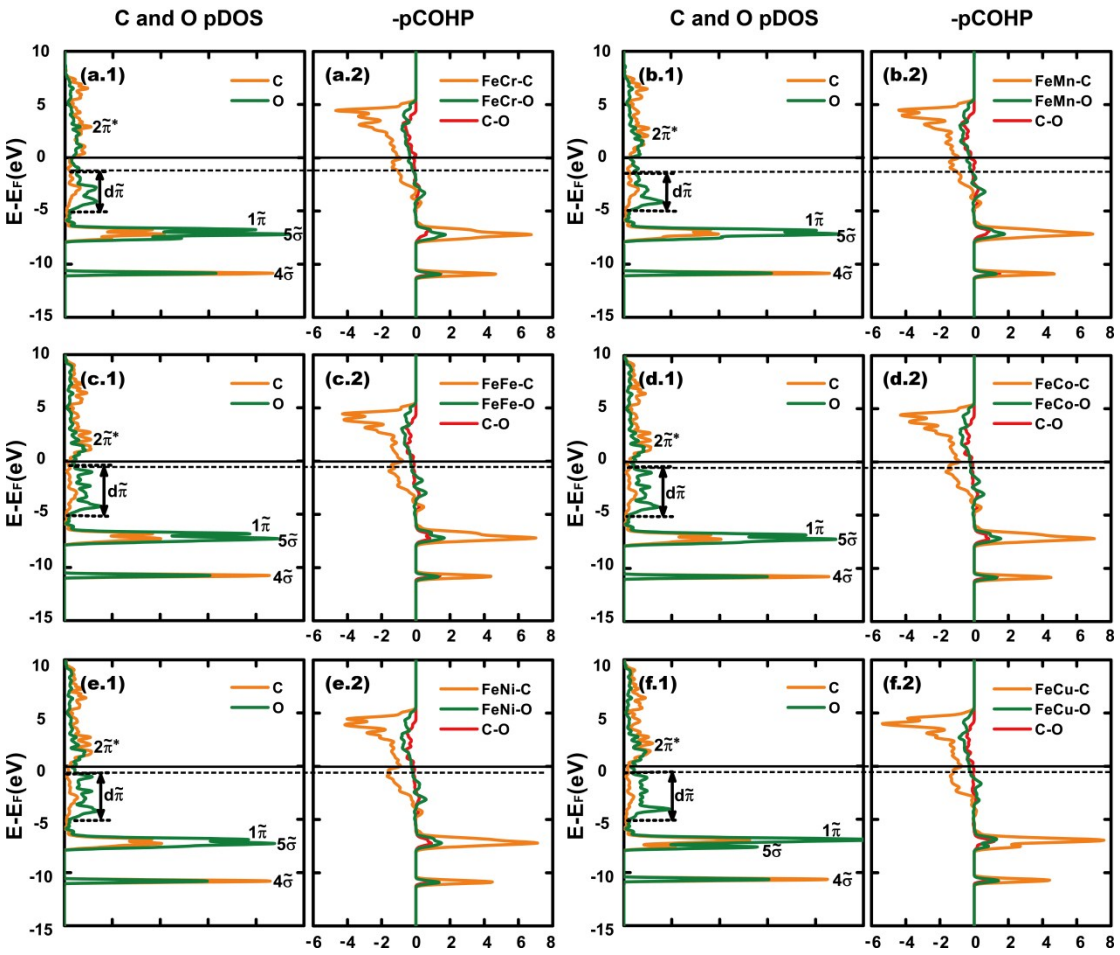

Fig. S5 PDOS and pCOHP curves for CO adsorption IS on pure and M–doped Fe(100) surfaces. The pDOS and pCOHP curves for Cr / Mn / Fe / Co / Ni / Cu doped site are shown in (a.1 / a.2), (b.1 / b.2), (c.1 / c.2), (d.1 / d.2), (e.1 / e.2), (f.1 / f.2), respectively

Fig. S5 diagrammatizes the pDOS and pCOHP curves of adsorbed CO on the transition metal doped Fe(100) surfaces. It can be seen that the bonding interaction contributes from the $4\tilde{\sigma}$, $5\tilde{\sigma}$, $1\tilde{\pi}$, and $d\tilde{\pi}$ orbitals in the adsorbed CO molecule, while the antibonding interaction between the surface atoms and the C/O atoms is contributed by the $2\tilde{\pi}$* orbital. In combination with the pCOHP curves, the $4\tilde{\sigma}$, $5\tilde{\sigma}$, and $1\tilde{\pi}$ states can be identified as narrow bands in the pDOS of C and O at approximately

−10.8, −7.6, and −6.6 eV with respect to the Fermi level. The broaden $d\tilde{\pi}$ and $2\tilde{\pi}^*$ bands are present in the range from −5 to 0 eV and around the Fermi level, respectively. It is greatly interesting to analysis the $d\tilde{\pi}$ and $5\tilde{\sigma}$ bands, which is relevant to the adsorption strength. Though the change is not obvious, due to only one atom is doped, slight differences also can be found. From the pDOS on the Cr–doped Fe(100) surface (**Fig. S5 a.1**), we found that the $5\tilde{\sigma}$ band and the center of $d\tilde{\pi}$ is lower than others, which result in the stronger adsorption energy (–2.45 eV). On the Cu–doped Fe(100) surfaces, the intensity of $5\tilde{\sigma}$ is weakened and thus adsorption strength is decreased (–1.97 eV).

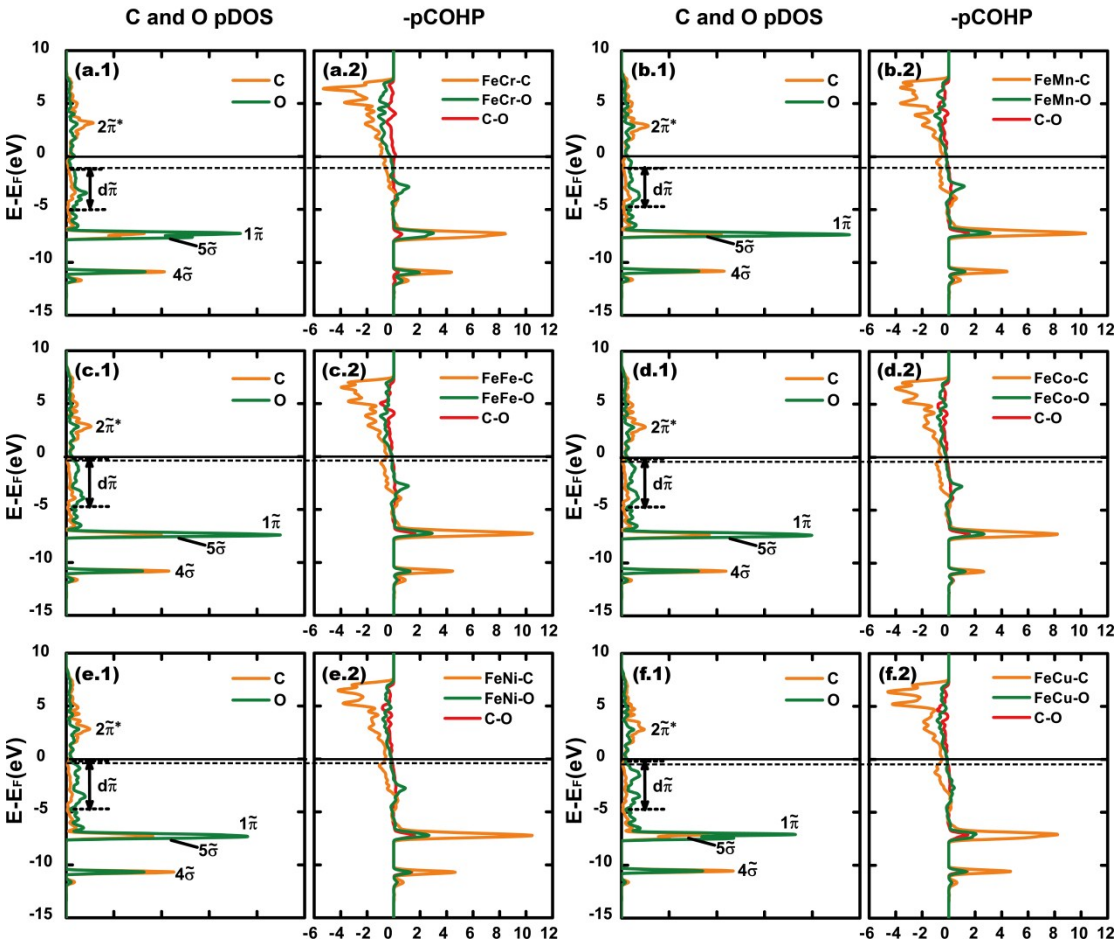

Fig. S6 PDOS and pCOHP curves for CO adsorption IS on pure and M–doped Fe_5C_2(100) surfaces. The pDOS and pCOHP curves for Cr / Mn / Fe / Co / Ni / Cu

doped site are shown in (a.1 / a.2), (b.1 / b.2), (c.1 / c.2), (d.1 / d.2), (e.1 / e.2), (f.1 / f.2), respectively

Fig. S6 shows the pDOS and pCOHP curves for adsorbed CO on the transition metal doped $Fe_5C_2(100)$ surfaces. The state of $4\tilde{\sigma}$ and overlap states of $5\tilde{\sigma}$ and $1\tilde{\pi}$ can be identified in the C and O pDOS at approximately −10.8, and −7.4 eV, respectively, with respect to the Fermi level. The broad $d\tilde{\pi}$ and $2\tilde{\pi}^*$ bands are also present in the range from −5 to 0 eV and around the Fermi level, respectively. Even though the pDOS and pCOHP curves are very similar, the center of $d\tilde{\pi}$ is found to be slightly raised from Mn–doped to Cu–doped surface. Furthermore, the polarization of oxygen in $d\tilde{\pi}$ is increased gradually from Mn–doped to Cu–doped, which indicates that the electron density shifted from oxygen to metal decreased and disabled the system, as illustrated in metal–O curve of pCOHP. These reasons result in the decreasing adsorption strength.